Analysis of RF Reflection Method for MOSFET Electrometer Fabricated by Standard Integrated-Circuit Technology

International Journal of ChemTech Research
CODEN (USA): IJCRGG ISSN: 0974-4290
Vol.7, No.3, pp 1623-1627, 2014-2015

ICONN 2015 [4th - 6th Feb 2015]
International Conference on Nanoscience and Nanotechnology-2015
SRM University, Chennai, India

Analysis of RF Reflection Method for MOSFET Electrometer Fabricated by Standard Integrated-Circuit Technology

Hiroshi Inokawa*, Mitsuru Kawai and Hiroaki Satoh

Research Institute of Electronics, Shizuoka University
3-5-1 Johoku, Naka-ku, Hamamatsu, 432-8011 Japan

Abstract: In this study, we characterized metal-oxide semiconductor field-effect transistor (MOSFET) electrometers by radio-frequency (RF) reflection method, in which the MOSFET constitutes the loss term of an LC tank circuit connected at the end of the transmission line, and the charge signal is detected as the change in the reflectance of the RF carrier signal. By this method, we can attain high-speed operation free from the constraint set by the output resistance and the cable capacitance, and high sensitivity not limited by the low-frequency flicker noise. It was demonstrated that a bulk MOSFET electrometer fabricated by the standard 65-nm process technology could operate at room temperature with a charge sensitivity of 1.7×10^{-3} e/√Hz for charge signal frequency of 3 MHz. It was also found that the down scaling of the gate length and the proper choice of the LC tank circuit parameters were important for obtaining the better charge sensitivity.
Keywords: Metal-oxide semiconductor field-effect transistor (MOSFET), Radio-frequency (RF) reflection method, Electrometer, Charge sensitivity.

Introduction

Highly sensitive electrometers are required for the readout of qubit states[1] and many other applications in sensing such as single-photon detection[2,3,4]. Although single-electron transistors (SET) have been researched for such applications[5], metal-oxide semiconductor field-effect transistors (MOSFETs) can now attain a charge sensitivity in the order of 10^{-3} e/√Hz at room temperature due to the aggressive down scaling[6], though the operation speed is rather low (~1 Hz). Considering the high-temperature and high-voltage operation as compared with the counterpart, and the ease of manufacturing by integrated-circuit technologies, MOSFET electrometers must have a wide range of usage. In this report, we will focus on the analysis by radio-frequency (RF) reflection, expecting a high-speed operation free from the constraint set by the output resistance and the cable capacitance, and high sensitivity not limited by the low-frequency flicker noise[7,8].

Experimental

Figure 1 shows the circuit diagram for the RF reflectance measurement. LC tank circuit including the MOSFET electrometer is connected at the end of the 1-m coaxial cable, and the reflected signal is separated by the directional coupler, and is monitored by the spectrum analyzer. An n-channel MOSFET with a gate length L_E=70 or 300 nm and a channel width W_E=110 nm fabricated by 65-nm bulk complementary metal-oxide semi

conductor (CMOS) process is used as an electrometer. In order to assure negligible gate leakage current, 5-nm gate oxide is used, and the inversion-layer extended source/drain is adopted to suppress short-channel effects[9]. Thanks to this device structure, high-sensitivity electrometer can be manufactured by the standard integrated-circuit technology.

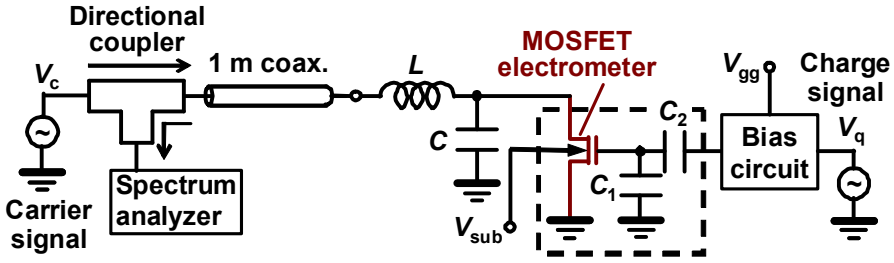

Fig. 1. Circuit diagram for RF reflectance measurement. Pad capacitance C, stray capacitance around MOSFET gate C_1 and coupling capacitance C_2 are 2 pF, 1.4 fF and 260 aF, respectively.

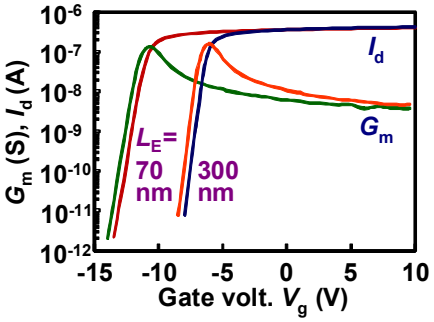

Fig. 2. Transfer characteristics of the electrometer MOSFETs with different gate lengths. Gate voltage V_g is applied via coupling capacitor C_1. Drain voltage is 50 mV.

In the measurement, substrate voltage (V_{sub}<0) is applied to accommodate AC signal in the drain. As indicated in Fig. 1, the MOSFET includes a stray capacitance C_1 in the gate wiring, and the charge signal ΔQ induced in the channel (in the unit of electron) is calculated from V_q considering the C_1 and the coupling capacitance C_2. Note that, although the circuit configuration in Fig. 1 is basically the same as that of RF-SET[10], voltage of the carrier signal can be increased more than that for the SET, resulting in an improved signal-to-noise ratio (SNR) and elimination of the cooled preamplifier.

Results and Discussion

Figure 2 shows the transfer characteristics of the electrometer MOSFETs with gate lengths L_E of 70 and 300 nm. Even with a relatively thick gate oxide of 5 nm, the device keeps the steep subthreshold slope for L_E=70 nm thanks to the shallow inversion-layer source/drain[9]. However, the transconductance G_m is barely improved at the shorter L_E because of the large series resistance in the inversion-layer source/drain. Therefore, the improvement in charge sensitivity for the shorter L_E is brought about only by the smaller input capacitance.

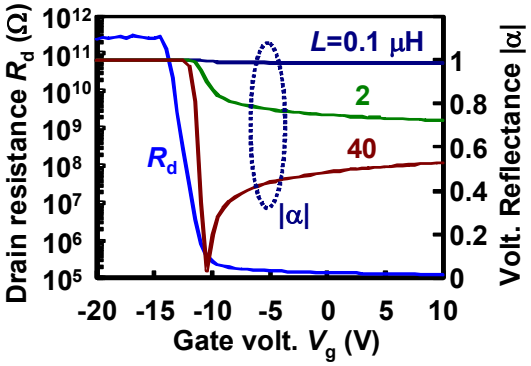

Fig. 3. Drain resistance R_d of the electrometer MOSFET with L_E=70 nm, and the calculated RF reflectance |α| for the tank circuit C=2 pF and various L's. The resonance frequencies for L=0.1, 2 and 40 μH are 360, 80 and 18 MHz, respectively.

Figure 3 shows the gate voltage dependence of the drain resistance R_d, and the RF voltage reflectance |α| for various tank circuit L's calculated by[11,12].

$$\alpha=(Z-Z_o)/(Z+Z_o). \quad (1)$$

Here, Z_o=50 Ω is the characteristic impedance of the coaxial cable, and Z is the impedance of the LC tank circuit including the R_d of the MOSFET electrometer given by

$$Z=i\omega L+(i\omega C+1/R_d)^{-1}. \quad (2)$$

The angular frequency ω (or frequency f) of the RF carrier signal is set at the resonance point

$$\omega=2\pi f=(LC)^{-1/2}. \quad (3)$$

The R_d changes largely over six orders of magnitude, but bottoms out at around 10^5 Ω. Even for such a large R_d, appreciable change in |α| can be obtained by properly selecting the L. Note that, if the L is excessively large, e.g. L=40 μH, the turning point[13] appears in |α|, and the frequency of the charge signal is also limited by the low resonance frequency.

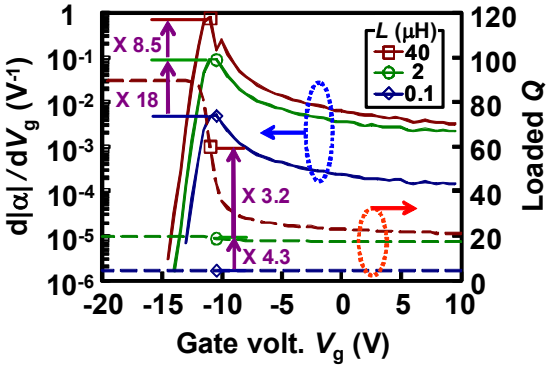

Fig. 4. d|α|/dV_g and the loaded quality factor Q as a function of V_g. d|α|/dV_g is proportional to the intensity of charge signal in the reflected RF spectrum. The Q is proportional to the drain voltage amplified by the LC tank circuit.

Figure 4 shows the d|α|/dV_g, which is proportional to the level of the charge signal in the reflected RF spectrum, and the loaded quality factor Q given by[11,12].

$$Q=[(L/C)^{-1/2}Z_o+(L/C)^{1/2}/R_d]^{-1}. \quad (4)$$

The Q is proportional to the drain voltage amplified by the LC tank circuit. If the L is increased from 0.1 to 2 μH, the reflected charge signal increases by a factor 18, but the amplitude of the carrier signal should be reduced by a factor 4.3 in order to keep the drain voltage lower than its upper limit. Therefore, the net

improvement in SNR is expected to be 4.2 (=18/4.3). In the same manner, the improvement by the change from L=2 to 40 μH is 2.7, although the d|α|/dV_g, shows an unnatural dip at around V_g= −10 V corresponding to the turning point in |α|. Considering the expected characteristics in Figs. 3 and 4 for different L's, we experimentally verified the cases for L=0.1 and 2.2 μH

Figure 5 shows the frequency spectra of the reflected signal for different levels of input charge signal ΔQ. On both sides of the central carrier signal, charge signals appear 3 MHz away from the center, reflecting the frequency of the input charge signal. Since the levels of the charge signal in the spectra are proportional to the input ΔQ, the signals are properly identified. SNR can be obtained as the charge signal level above the noise floor, and the charge sensitivity δq, i.e. the minimum detectable charge, can be calculated by

$$\delta q = \Delta Q/\mathrm{SNR}/\mathrm{RBW}^{1/2}. \qquad (5)$$

Here, RBW is the resolution band width of the spectrum analyzer.

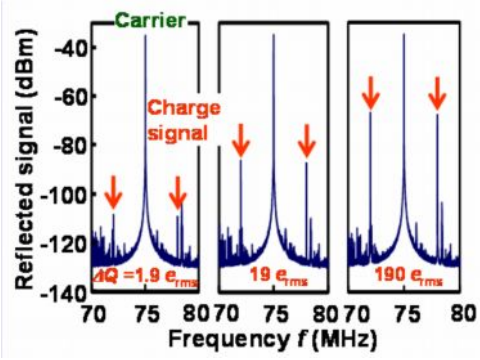

Fig. 5. Frequency spectra of the reflected signal for L=2.2 μH, L_E = 70 nm, V_c = −10 dBm, and RBW=3 kHz. ΔQ is the charge induced in the MOSFET channel by the input V_q. Charge signal in the spectra is proportional to the ΔQ.

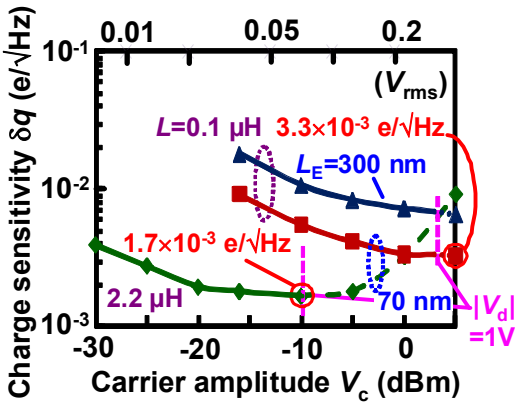

Fig. 6. Charge sensitivity as a function of the carrier amplitude for different gate lengths L_E of the electrometer MOSFET and different L's of the tank circuit.

Figure 6 shows the charge sensitivity as a function of the carrier amplitude V_c for different L_E's and L's. The charge sensitivity is improved as the carrier amplitude increases due to the improved SNR, but it saturates at the V_c corresponding to the drain voltage |V_d|=1 V, i.e. V_c=3 dBm for L= 0.1 μH and V_c= −10 dBm for L=2.2 μH as indicated by the vertical dashed lines in Fig. 6. The |V_d| is limited by the substrate voltage V_{sub}= −1 V in order to prevent the forward biasing of the drain-substrate junction. The reduction of the MOSFET gate length L_E is also found to be effective in improving the charge sensitivity. The best sensitivities for L= 0.1 and 2.2 μH are 3.3 and 1.7 × 10^{-3} e/√Hz, respectively. Although these values are behind those of SETs [10,11,12,13], it is practically important that the MOSFET electrometer can operate at room temperature. Compared to the reported

MOSFET electrometer with an operation speed of ~1 Hz[6], the merit of the high-speed operation by the RF reflectance method is obvious. Moreover, the device shown here can be made in a bulk silicon substrate by the common CMOS process, and does not require special structure or silicon-on-insulator substrate[6,8].

Conclusion

By the use of the RF reflection method, a MOSFET electrometer fabricated by standard integrated-circuit technology with a gate length of 70 nm could operate at room temperature with a charge sensitivity of 1.7×10^{-3} e/√Hz and charge signal frequency of 3 MHz. It was also found that the down scaling of the gate length and the proper choice of the LC tank circuit parameters are important for obtaining the better charge sensitivity.

Acknowledgement

Authors are deeply indebted to Keisaku Yamada of University of Tsukuba, Toyohiro Chikyo of National Institute of Materials and Science, Tetsuo Endoh of Tohoku University, Hideo Yoshino and Shigeru Fujisawa of Semiconductor Leading Edge Technologies, Inc. for their cooperation in the device fabrication. They also thank Murata Manufacturing Co., Ltd. for providing chip inductors. This research was supported by Japan Society for the Promotion of Science Grant-in-Aid for Scientific Research 25286068.

References

1. Gorman J., Hasko D. G., and Williams D. A., Charge-Qubit Operation of an Isolated Double Quantum Dot, Phys. Rev. Lett., 2005, 95, 090502_1-4.
2. Du W., Inokawa H., Satoh H., and Ono A., SOI metal-oxide-semiconductor field-effect transistor photon detector based on single-hole counting, Optics Letters, 2011, 36, 2800-2802.
3. Du W., Inokawa H., Satoh H., and Ono A., Single-Photon Detection by a Simple Silicon-on-Insulator Metal-Oxide-Semiconductor Field-Effect Transistor, Jpn. J. Appl. Phys., 2012, 51, 06FE01_1-4.
4. Putranto D. S. C., Priambodo P. S., Hartanto D., Du W., Satoh H., Ono A., and Inokawa H., Effects of substrate voltage on noise characteristics and hole lifetime in SOI metal-oxide-semiconductor field-effect transistor photon detector, Optics Express, 2014, 22, 22072-22079.
5. Likharev K. K., Single-Electron Devices and Their Applications, Proc. IEEE, 1999, 87, 606- 632.
6. Nishiguchi K., Koechlin C., Ono Y., Fujiwara A., Inokawa H., and Yamaguchi H., Single-Electron-Resolution Electrometer Based on Field-Effect Transistor, Jpn. J. Appl. Phys., 2008, 47, 8305-8310.
7. Kawai M., Singh V., Nagasaka M., Hiroaki Satoh H., and Inokawa H., Analysis of MOSFET Electrometer Sensitivity by Radio-Frequency Reflection, Int. Conf. Solid State Devices and Materials (SSDM), Tokyo, Japan, Sept. 22-24, 2010, P-9-13, 491-492.
8. Nishiguchi K., Yamaguchi H., Fujiwara A., van der Zant H. S. J., and Steele G. A., Wide-bandwidth charge sensitivity with a radio-frequency field-effect transistor, Appl. Phys. Lett., 2013, 103, 143102_1-4.
9. Singh V., Inokawa H., Endoh T., and Satoh H., Fabrication Method of Sub-100 nm Metal-Oxide-Semiconductor Field-Effect Transistor with Thick Gate Oxide, Jpn. J. Appl. Phys., 2010, 49, 128002_1-2.
10. Schoelkopf R. J., Wahlgren P., Kozhevnikov A. A., Delsing P., and Prober D. E., The Radio-Frequency Single-Electron Transistor (RF-SET): A Fast and Ultrasensitive Electrometer, Science, 1998, 280, 1238-1242.
11. Turin V. O. and Korotkov A. N., Analysis of the radio-frequency single-electron transistor with large quality factor, Appl. Phys. Lett., 2003, 83, 2898-2900.
12. Turin V. O. and Korotkov A. N., Numerical analysis of radio-frequency single-electron transistor operation, Phys. Rev. B, 2004, 69, 195310_1-13.
13. Fujisawa T. and Hirayama Y., Transmission Type RF Single Electron Transistor Operation of a Semiconductor Quantum Dot, Jpn. J. Appl. Phys., 2000, 39, 2338-2340.

***** *****